Scientific Reports

https://doi.org/10.1038/s41598-026-45960-w

Article in Press

Combining network pharmacology and experimental validation to study the action and mechanism of brusatol against lung adenocarcinoma

Received: 8 October 2025

Accepted: 23 March 2026

Published online: 03 April 2026

Cite this article as: Jin X., Yang S., Pan D. *et al.* Combining network pharmacology and experimental validation to study the action and mechanism of brusatol against lung adenocarcinoma. *Sci Rep* (2026). https://doi.org/10.1038/s41598-026-45960-w

Xin Jin, Shixiong Yang, Dianzhu Pan, Bo Jin, Ye Zhang & Chunjiao Yang

Combining Network Pharmacology and Experimental Validation to Study the Action and Mechanism of Brusatol Against Lung Adenocarcinoma

Xin Jin[1#]，Shixiong Yang[2#]， Dianzhu Pan[3]，Bo Jin[4]，Ye Zhang[4]，Chunjiao Yang[5*]

[1] Department of Respiratory Medicine, The Fifth Affiliated Hospital of Guangxi Medical University & The First People's Hospital of Nanning, Nanning, Guangxi, China.

[2] The Fifth Affiliated Hospital of Guangxi Medical University & The First People's Hospital of Nanning, Nanning, Guangxi, China.

[3] The Jinzhou Medical University，Jinzhou，Liaoning，China

[4]The First Affiliated Hospital of China Medical University，Shenyang, Liaoning, China.

[5] Department of Oncology, The Fifth Affiliated Hospital of Guangxi Medical University & The First People's Hospital of Nanning, Nanning, Guangxi, China.

*** Correspondence:**
Corresponding Author：Chunjiao Yang
yangchunjiao@163.com

These authors contributed equally

Keywords: Lung adenocarcinoma[1], Chinese medicine[2], Network pharmacology[3], Brusatol[4], Ras signaling pathway[5].

Abstract

Brusatol is a natural product found in the plant *Brucea javanica* that is used to treat diseases such as amoebiasis and malaria. It also has significant anti-tumor effects. However, its role in lung cancer and the mechanism underlying its pharmacological effects remain unclear. In this study, we identified the core target of brusatol for lung adenocarcinoma (LUAD) therapy using network pharmacology and elucidated its therapeutic mechanism by conducting cell experiments. The therapeutic targets of brusatol were obtained from the PharmMapper database, the LUAD-related genes were obtained from the TCGA database, and the intersection targets of the two were taken as potential targets for treating LUAD with brusatol. Based on the results of the intersection, core target and signaling pathways were identified by protein-protein interaction (PPI), molecular docking, gene ontology (GO) function, and Kyoto Encyclopedia of Genes and Genomes (KEGG) pathway enrichment analyses. Finally, cell experiments were performed to determine the antineoplastic effect of brusatol on LUAD. We identified

328 potential targets of brusatol for treating LUAD, and the PPI network analysis identified ALB, SRC, HSP90AA1, HRAS, CASP3, MAPK1, and ESR1 as key genes. Through molecular docking, MAPK1 was identified as the core target of brusatol in LUAD. GO analysis revealed that brusatol may exert anti-tumor effects through endopeptidase activity, protein tyrosine kinase activity, and amide binding. KEGG enrichment analysis suggested that brusatol may treat LUAD by regulating the RAS signaling pathway. Brusatol inhibited the proliferation and invasion of LUAD cells and caused apoptosis and G2/M phase arrest in these cells. Further analysis confirmed that brusatol plays a role in treating LUAD by targeting MAPK1 and regulating the Ras signaling pathway. To summarize, through a combination of network pharmacological analysis and cell experimental validation, we revealed the mechanism underlying the therapeutic effects of brusatol on LUAD. This study also provided a theoretical basis for using brusatol as a candidate drug for the targeted therapy of LUAD.

1 Introduction

Lung cancer is one of the most common causes of cancer-related death, with more than 1.8 million deaths recorded worldwide in 2021 [1]. Over the past decade, with the development of medical technology, the mode of treatment, including chemotherapy, targeted therapy, and immunotherapy, along with surgery, has changed considerably[2,3]. However, the five-year overall survival time for patients with lung cancer is still less than 20%. Moreover, for patients with advanced lung cancer, the adverse effects of chemotherapy, such as nausea, vomiting, and bone marrow suppression, are often quite severe and can even lead to the discontinuation of treatment[4]. Traditional Chinese medicine (TCM) is often accepted for treating tumors because of its reliable efficacy and extremely low adverse effects. Therefore, the development of new Chinese anticancer medicines is becoming increasingly important for treating lung cancer.

In China, TCM has played an irreplaceable role in human health and disease treatment. Owing to the particularity and integrity of TCM, the mechanism of action of many herbs is unknown. In 2007, British researchers first proposed the concept of "network pharmacology" and proposed "a new model for the next generation of drug research and development"[5,6]. Several researchers determined the mechanism of action of danshen against anemia using network pharmacology[7]. In the field of oncology, researchers have used network pharmacology to analyze the active constituents of *Prunella vulgaris* L. by screening its targets and further revealing its molecular mechanism in the treatment of breast cancer[8]. Moreover, researchers have applied network pharmacology and

molecular docking to predict the mechanism of scopoletin in treating non-small cell lung cancer (NSCLC)[9].

Researchers frequently use the anti-tumor mechanism of TCM monomers. Paclitaxel and vincristine are commonly used anticancer drugs in clinical practice, and they are derived from TCM. Brusatol was isolated and extracted from the seeds of *Brucea javanica* in 1968, when it was used to treat diseases such as amoebiasis and malaria. Over the past few decades, as researchers have continued to explore, several studies have demonstrated the anti-tumor effects of brusatol[10]. In 1979, brusatol was first defined as an experimental drug for treating leukemia; it strongly inhibits the metabolism and proliferation of tumor cells both in vivo and in vitro [11]. Besides studies on hematologic tumors, some groundbreaking studies have shown that brusatol is highly effective in solid tumors. For example, the cytotoxic effects of brusatol can induce the death of pancreatic cancer cells[12]. Brusatol downregulates the protein expression of HIF-1α and c-myc and inhibits the progression of colorectal cancer [13]. Brusatol can inhibit the growth of glioma [14], hepatocellular carcinoma [15], and melanoma [16] by regulating the expression of the NRF2 protein. However, studies on the anti-tumor effects of brusatol on lung adenocarcinoma (LUAD) are rare.

In this study, we predicted the molecular mechanism underlying the therapeutic effects of brusatol on LUAD by conducting network pharmacology and molecular docking analyses, and elucidated this mechanism by conducting cell experiments. We found that brusatol plays a role in various biological behaviors of LUAD cells. We also discussed recent findings concerning the molecular targets of brusatol and its value in cancer therapy (Figure 1).

2 Materials and Methods

2.1 Network Pharmacology

The chemical structure of brusatol was downloaded from the PubChem database(https://pubchem.ncbi.nlm.nih.gov/). The potential targets of Brusatol were obtained from three databases: PharmMapper(http://lilab-ecust.cn/pharmmapper/)(Norm Fit > 0.3), SwissTargetPrediction(https://www.swisstargetprediction.ch/)(Probability > 0.1), and ChEMBL(https://www.ebi.ac.uk/chembl/). The complete list of targets is provided in Supplementary Table 1. The potential targets for Lung Adenocarcinoma (LUAD) were obtained from two databases: TCGA (https://portal.gdc.cancer.gov/) and GenCLiP 3 (http://cismu.net/genclip3/analysis.php). From TCGA, we downloaded data from 589 LUAD samples (530 tumor tissues and 59 normal

controls). Differential expression analysis was performed using the limma package[17] in R, with the cutoff criteria set at |log2(Fold Change)| > 1 and adjusted p-value < 0.05. The complete list of targets is provided in Supplementary Table 2. The Venny 2.1 platform (https://bioinfogp.cnb.csic.es/tools/venny/index.html) was used to obtain the intersection targets between brusatol and the targets related to LUAD.

The STRING platform (https://cn.string-db.org/) was used to construct a protein-protein interaction (PPI) network for brusatol-related and LUAD-related potential targets with a medium confidence level (0.7). To hide disconnected nodes in the network, the Cytoscape V3.8.0 (http://www.cytoscape.org/) software was used to analyze the topology and calculate the degree value of each node. The R software was used (filter set to "p value cutoff = 0.05 and q value cutoff = 0.05") for gene ontology (GO) analysis and Kyoto Encyclopedia of Genes and Genomes (KEGG) pathway analysis[18–20]. High-resolution "*Homo sapiens*" three-dimensional protein structures of core targets were obtained from the Protein Data Bank (PDB) (http://www.rcsb.org/pdb/). Schrodinger Suites software was used to simulate computer methods to predict the relationship between brusatol and the target.

2.2 Experimental Validation

2.2.1 Preparation of Brusatol

Brusatol (**Figure 2A**, formula: $C_{26}H_{32}O_{11}$) was purchased from MedChemExpress (MCE). Mother liquors formulated with ddH_2O as a solvent can be diluted directly with a medium to the desired working solution concentration. Storage temperature: –80 °C, six months; –20 °C, one month.

2.2.2 Cell Culture

We purchased LUAD cell lines (A549 and H1299) from the Shanghai Institute of Cell Biology, Chinese Academy of Sciences. The cells were cultured in 1640 medium (RPMI1640, BI, 01-100-1ACS) supplemented with 1% penicillin-streptomycin (PS, Beyotime, C0222) and 10% fetal bovine serum (FBS, BI, 04-001-1B) at 37 °C in a 5% CO_2 atmosphere.

2.2.3 Cell Viability Assay

Initially, A549 and H1299 cells (100 µL/well; 1 × 103 cells/mL) were inoculated in a 96-well plate and cultured overnight in a humidified incubator at 37 °C and 5% CO_2. The cells were pretreated with different concentrations of brusatol (0, 10, 20, 40, 80, or 160 nM) for 24 h or 48 h. Then, 20 µL

of 3-(4,5)-dimethylthiahiazo (-z-y1)-3,5-di- phenytetrazoliumromide (MTT, Solarbio, 298–93-1) was added to each well, and the culture was incubated at 37 °C and 5% CO_2 for 4 h. Finally, the supernatant from each well was removed, 150 µL of dimethyl sulfoxide (DMSO, Solarbio, D8370) was added to each well, and the absorbance was measured using a microplate reader (Biotech, United States) at 490 nm.

2.2.4 Colony Formation Assay

We inoculated LUAD cells in a six-well plate at a density of 80 cells per well. A549 and H1299 cells were pretreated with 0, 20, 40, or 80 nM brusatol for 24 h, respectively. The cells were cultured in fresh 1640 medium in the absence of brusatol and then cultured for 14 days. When the colonies were visible to the naked eye, the culture was terminated. The colonies were washed with PBS buffer, fixed with methanol, stained with crystalline violet solution, and imaged under a microscope.

2.2.5 Cell Cycle Analysis via Flow Cytometry

First, LUAD cells at the logarithmic growth stage were inoculated in a six-well plate, and the supernatant was discarded after the cells adhered to the wall. The cells were pretreated with 0, 20, 40, or 80 nM brusatol for 24 h. Then, the cells were digested with trypsin and washed with precooled PBS. The cell density was calculated under a microscope, and the collected LUAD cells (1×10^6 cells) were fixed in precooled 70% ethanol and stored for 2 h at 4 °C. Finally, 500 µL of propidium iodide (PI) reagent was added to each sample following the protocol provided with the cell cycle kit (Thermo Fisher, F10797). The results were analyzed using a flow cytometer (BD Accuri™ C6 Flow Cytometer, United States) and the Modifit 5.0 software.

2.2.6 Determination of Cell Apoptosis via Flow Cytometry

Initially, A549 and H1299 cells (1×10^5 cells/mL) were cultured in six-well plates for 24 h and then treated with 0, 20, 40, or 80 nM brusatol for 24 h. LUAD cells were treated following the instructions provided with the Apoptosis Detection Kit (Beyotime, C1062M), and the Annexin V-FITC and PI reagents were added to each sample and incubated for 15 min in the dark. The results were analyzed using a flow cytometer (BD, United States).

2.2.7 Transwell Invasion Assay

An 8 µm well Transwell chamber system (Corning 3422, United States) was used to perform the Transwell invasion assay. The Matrigel matrix gel (BD, 356234) was coated onto the upper chamber.

A549 and H1299 cells (1×10^4 cells/mL) were inoculated in the upper chamber, supplemented with 200 μL of FBS-free medium, and treated with 0, 20, 40, or 80 nM brusatol for 24 h. Complete medium (600 μL) containing 10% FBS was added to the lower chamber. After 24 h, the culture was terminated, the cells were stained with crystal violet solution, photographed under a microscope, and counted.

2.2.8 Western Blotting Analysis

After extracting cellular proteins, the instructions for the SDS-PAGE Gel Preparation Kit (Beyotime, P0012A) were followed to separate and transfer equal amounts of protein to a polyvinylidene fluoride (PVDF) membrane (Millipore, IPVH00010). The PVDF membranes were blocked with blocking buffer (NCM, P30500) for 10 min at room temperature and then incubated with primary antibodies overnight at 4 °C. The following day, the PVDF membranes were washed with TBST (Solarbio, T1082) three times (10 min per wash) and then incubated with goat anti-rabbit horseradish peroxidase (HRP)-conjugated secondary antibodies for 1 h at room temperature. Finally, the protein bands were visualized with an enhanced chemiluminescence (ECL) luminescence kit (Beyotime, P0018AS). The antibodies used were as follows: anti-Bax (Proteintech, 50599-2-lg), anti-Bcl2 (Proteintech, 12789-1-AP), anti-Cyclin B1 (Proteintech, 28603-1-AP), anti-P21(ZENBIO, 381102), anti-p-cdc2 (Tyr15) (ZENBIO,310063), anti-cdc2 (abcam,ab32094), anti-Caspase3/p17/p19 (Proteintech,19677-1-AP), anti-MMP9 (Proteintech,10375-2-AP), anti-E-cadherin (Proteintech,60335-1-Ig), anti-vimentin (Proteintech, 60330-1-Ig), anti-MEK1/2 (Proteintech, 11049-1-AP), anti-p-ERK1/2 (ZENBIO, 301245), anti-MEK1/2 (Proteintech, 11049-1-AP), anti-p-MEK1/2 (Abcam, ab4750), anti-Raf (Abcam, ab200653), anti-p-Raf (Abcam, ab173539), and anti-β-actin 1:1,000 (Cell Signaling Technology, 3700), goat anti-rabbit HRP-coupled secondary antibodies 1:5,000 (Proteintech, SA00001-2).

2.2.9 Statistical Analysis

All data were visually and statistically analyzed using GraphPad Prism 8.0 and the R software. The differences among multiple groups were determined by conducting one-way analysis of variance (ANOVA), and those between groups were determined by conducting Student's t-tests. All data were presented as the mean ± SD. All differences among and between groups were considered to be statistically significant at $p < 0.05$. All experiments were repeated in triplicate.

3 Results

3.1 Network Pharmacological Analysis of Brusatol for the Treatment of LUAD

To systematically identify potential therapeutic targets of Brusatol in Lung Adenocarcinoma (LUAD), we first predicted Brusatol-related targets using three databases—PharmMapper, SwissTargetPrediction, and ChEMBL—yielding 409 unique targets. Next, we analyzed transcriptomic data from the TCGA database, comparing 530 LUAD tumor tissues with 59 normal controls, and identified 6,380 differentially expressed genes ($|\log2FC| > 1$, adjusted $p < 0.05$). Additionally, we retrieved 4,872 LUAD-associated genes from the GenCLiP 3 database. The union of these two gene sets (TCGA and GenCLiP 3) resulted in 9,510 LUAD-related targets. Finally, by intersecting the Brusatol targets (n = 409) with the LUAD-associated genes (n = 9,510), we identified 292 overlapping targets, which may represent potential key mediators of Brusatol's anti-LUAD effects(**Figure 2B**). A total of 292 intersecting genes were introduced into the STRING online platform to construct a target PPI network (the selected species was *Homo sapiens*, confidence level >0.7). A total of 292 candidate targets were introduced into the Cytoscape 3.8.0 software, and a visualized target network was constructed. The degree value of each node was calculated by conducting topological analysis, and the degrees of the first 40 target genes are shown in **Table 1**. The results of the visual analysis are shown in **Figure 2C**. We identified the genes ALB, SRC, HSP90AA1, HRAS, CASP3, MAPK1, and ESR1 with a degree >150 as key genes for treating LUAD with brusatol. These key genes may contribute to the fundamental therapeutic role of brusatol in LUAD.

Molecular docking analysis was performed to validate the binding modes of these seven key genes with brusatol. We found that MAPK1, CASP3, SRC, ESR1, and HRAS directly bound to brusatol (**Figure 2D**). ALB and HSP90AA1 did not directly bind to brusatol. A lower binding energy indicates greater stability. The binding energies between MAPK1, CASP3, SRC, ESR1, HRAS, and brusatol were –5.418, –4.107, –3.715, –2.47, and –2.384 kJ/mol, respectively (**Table 2**). The results indicated that brusatol could bind to the active sites of the targets. MAPK1 may become a core target for brusatol in the treatment of LUAD because of its high stability in binding to brusatol.

To predict the mechanism underlying the therapeutic effect of brusatol on LUAD, the R software was used to conduct enrichment analysis of the GO and KEGG pathways[21–23]. A total of 70 results that met the criteria were screened ($p < 0.05$). The top 20 significantly enriched GO terms were plotted on the left side of **Figure 2E**, and these results suggested that brusatol might exert its anticancer effects on LUAD through endopeptidase activity, protein tyrosine kinase activity,

phosphatase binding, and amide binding. A total of 151 signaling pathways were obtained by KEGG enrichment analysis. The first 20 significant signaling pathways with high confidence and $p < 0.05$ were selected for visualization. Many genes were found to be associated with endocrine and immune functions, including the insulin signaling pathway, neurotrophin signaling pathway, and IL-17 signaling pathway (**Figure 2F**). However, we focused on cancer-related signaling pathways. We also found that most target genes were associated with signaling pathways involved in cancer development, including the Ras signaling pathway, the VEGF signaling pathway, the PPAR signaling pathway, and the T-cell receptor signaling pathway.

3.2 Brusatol Inhibited the Proliferation of LUAD Cells

Initially, A549 and H1299 cells were treated with different concentrations of brusatol (0, 10, 20, 40, and 80 nM) for 24 h or 48 h. The results of the MTT assay revealed that brusatol inhibited the proliferation of NCSLS cells in a time-dependent and dose-dependent manner (**Figure 3A**). The 24 h and 48 h IC50 values of brusatol for A549 cells were 57.04 nM and 36.06 nM, respectively. The 24 h and 48 h IC50 values of brusatol for H1299 cells were 60.62 nM and 38.92 nM, respectively. We performed further experiments with a 1/2 IC50 value, an IC50 value, and two times the IC50 value; the results strongly suggested that brusatol has cytotoxic effects.

We evaluated the effects of brusatol on the proliferation of LUAD cells (A549 and H1299) by conducting a colony formation assay. We found that different concentrations (0, 20, 40, and 80 nM) of brusatol inhibited colony formation in a dose-dependent manner (**Figure 3B**). These findings indicate that brusatol inhibits the formation of cell colonies and the proliferation of LUAD cells.

Compared to that of the control cells, the proportion of S-phase A549 and H1299 cells gradually decreased as the concentration of brusatol increased, whereas the proportion of G2/M-phase cells gradually increased (**Figure 3C**). Brusatol promoted the expression of p-cdc2 and P21 and inhibited the expression of Cyclin B1 proteins in A549 and H1299 cells (**Figure 3D**). These results demonstrated that brusatol inhibited the proliferation of LUAD cells.

3.3 Brusatol Promoted the Apoptosis of LUAD Cells

The effects of different concentrations (0, 20, 40, and 80 nM) of brusatol on the apoptosis of LUAD cells were determined by flow cytometry. The results revealed that the percentage of apoptotic A549 and H1299 cells increased significantly as the concentration of brusatol increased (**Figure 4A**).

Brusatol promoted the expression of Bax and cleaved caspase-3 and inhibited the expression of the Bcl-2 protein in A549 and H1299 cells (**Figure 4B**). These results indicate that brusatol has an apoptosis-inducing effect on LUAD cells.

3.4 Brusatol Inhibited the Invasion of LUAD Cells

Transwell invasion experiments were performed to evaluate the effect of brusatol on the invasion ability of A549 and H1299 cells. The results revealed that invasion of A549 and H1299 cells was inhibited in a dose-dependent manner in the brusatol-treated group (**Figure 5A**). Brusatol promoted the expression of E-cadherin and inhibited the expression of vimentin and MMP9 proteins in LUAD cells (**Figure 5B**). These results confirmed that brusatol inhibits the invasion of LUAD cells.

3.5 Mechanism Underlying the Therapeutic Effect of Brusatol on LUAD

Based on previous bioinformatics predictions (Figure 2D and Table 2), MAPK1 (also known as ERK2) was the core target of brusatol (**Figure 2E**), and the RAS signaling pathway was the key pathway. Therefore, we investigated whether brusatol targeted MAPK1 anti-tumor activity and whether the RAS signaling pathway was involved in the anti-tumor effects of brusatol.

We also investigated the mechanism underlying the therapeutic effects of brusatol on LUAD by conducting Western blotting analysis of LUAD cells. The results suggested that brusatol inhibited the expression of p-ERK1/2 in A549 and H1299 cells (**Figure 6A**). Brusatol affected the expression levels of key proteins in the RAS signaling pathway (**Figure 6B**). We found that increasing the brusatol concentration significantly decreased the levels of p-MEK1/2 and p-Raf. Moreover, following Brusatol treatment, we introduced the ERK activator pamoic acid. Results from colony formation assays, flow cytometry-based cell cycle analysis, and EdU incorporation assays consistently demonstrated that pamoic acid reversed the Brusatol-induced alterations in lung cancer cells(**Figure S1A-C**). To summarize, these findings supported the bioinformatics prediction that brusatol targets MAPK1 and modulates the RAS signaling pathway in the treatment of LUAD.

4 Discussion

Cancer is defined as the uncontrolled proliferation of cells, and oncogenes and tumor suppressor genes are often used as targets to inhibit cancer progression[21]. The ultimate goal of developing anticancer TCM is to accurately inhibit the growth of tumors. Owing to their safe tumor-inhibiting activity, natural product monomers in TCM plants are promising new options for treating cancer[23].

However, owing to the complexity of TCM, determining its mechanism of action is difficult. The emergence of network pharmacology in recent years has revealed new ways to overcome this problem. Characterized by predictability, network pharmacology emphasizes the multichannel regulation of signaling pathways to improve the precision of the therapeutic effect of drugs on diseases [24]. Online databases of biological information are used to comprehensively and systematically analyze the mechanisms underlying the anticancer effects of TCM. It emphasizes the interpretation of the molecular mechanism of drug treatment of diseases from the perspective of the whole body and the understanding of the whole process of pharmacokinetics from the perspective of a biological network. This provides more options and possibilities for the precise treatment of diseases, which coincides with the whole concept of the TCM system [25].

Brusatol-mediated expression of the NRF2 protein induces apoptosis in NSCLC [26]. Therefore, we applied network pharmacology to construct a relationship network of brusatol-LUAD. Through PPI network analysis, we identified 328 potential drug therapeutic targets, among which the key targets were ALB, SRC, HSP90AA1, HRAS, CASP3, MAPK1, and ESR1. To identify precise therapeutic targets, we performed molecular docking analysis to determine whether MAPK1 is the core target of brusatol in the treatment of LUAD. Some studies have shown that brusatol inhibits tumor growth by regulating the PI3K/AKT signaling pathway [27]. The results of our analysis revealed that the effects of brusatol in the treatment of LUAD are closely related to multiple signaling pathways. Among them, the signaling pathways highly correlated with cancer include the Ras signaling pathway, the VEGF signaling pathway, and the apoptosis signaling pathway. Combined with the identification of core targets, we speculated that brusatol may treat LUAD by regulating the Ras signaling pathway.

Several studies have shown that brusatol inhibits the growth of various tumors. Similarly, our study also revealed that brusatol was cytotoxic to LUAD cells and inhibited the proliferation of A549 and H1299 cells in a concentration-dependent manner. The cell cycle is a complex process, and disruption of the cell cycle is a key reason for the rapid growth of tumors [28]. The expression of the cycle-critical protein p21 can keep tumor cells in the G2/M phase [29]. Our results were consistent with this process. As brusatol concentration increased, the expression of the p21 protein increased, and the increase in p-cdc2 and decrease in the cyclin B1 protein decreased the number of complexes formed by the two proteins. Apoptosis is one of the causes of the unlimited growth of cancer [30]. Many researchers are developing new drugs for each step of apoptosis [31,32]. Studies have shown that brusatol induces the apoptosis of pancreatic cancer cells [12]. Additionally, brusatol can also

induce apoptosis in human gastric cancer cells [33]. Similar to the findings of these studies, our results also revealed that as the concentration of brusatol increased, the proportion of A549 and H1299 cells that underwent apoptosis increased. The expression of the pro-apoptotic protein Bax and the anti-apoptotic protein Bcl-2 showed an imbalance, and the expression of the protein cleaved-caspase-3, an executive molecule in the apoptosis process, increased. Metastasis is the leading cause of tumor-related death [34] and has become a hallmark of cancer [35]. Brusatol can inhibit the invasion of glioblastoma [36], laryngeal carcinoma [37], and hepatocellular carcinoma [38]. Our results suggest that brusatol can inhibit the invasion of LUAD cells in a dose-dependent manner. Moreover, brusatol altered key proteins involved in the invasion process, which was further demonstrated by the increase in the expression of the E-cadherin protein and the decrease in the expression of the proteins MMP9 and vimentin.

The uncertainty of the mechanism of action of brusatol has limited its entry into clinical practice and further development for a long time. MAPK1 is a member of the MAPK family and is a common carcinogen. MAPK1 is involved in the malignant biological behavior of various tumors, and high expression of MAPK1 can promote the migration and invasion of gastric cancer [39], NSCLC [40], and pancreatic cancer (PAAD) [22] while inhibiting their apoptosis. We speculated that blocking MAPK1 with small-molecule inhibitors may constitute a viable model for targeted cancer therapy. We found that brusatol inhibited the expression of the MAPK1 protein. MAPK1 is a key protein in the Ras signaling pathway. The Ras signaling pathway is involved in the regulation of several important cellular functions, such as proliferation, growth, and aging [41]. The Ras signaling pathway and its related proteins are dysregulated in nearly one-third of human cancers, and activation of Ras leads to the growth, differentiation, and survival of cells, ultimately leading to the occurrence of cancer [42,43]. These results indicate that brusatol inhibits the proliferation and invasion of cells, promotes G2/M phase arrest and apoptosis, and exerts a therapeutic effect on LUAD by targeting MAPK1, which mediates the Ras signaling pathway. Compared to the known targeted therapeutic agents, such as KRAS inhibitors (e.g., sotorasib), which focus primarily on specific KRAS mutations and face challenges such as drug resistance and limited applicability across different types of cancer, brusatol offers distinct advantages. First, as a natural product derived from TCM, brusatol acts via a multitarget mechanism by simultaneously modulating key nodes in the Ras pathway and related processes, such as apoptosis and cell cycle arrest, potentially reducing the chances of the development of resistance. Second, while KRAS inhibitors are often mutation-specific, the broad-spectrum activity of brusatol against multiple Ras-driven tumors may provide a wider therapeutic

window. Additionally, the ability of brusatol to integrate with systemic biological networks—aligning with the holistic philosophy of TCM—could improve its safety profile compared to that of synthetic targeted agents, which are frequently associated with off-target effects. Future studies should validate these comparative advantages in preclinical and clinical settings.

These results indicate that brusatol inhibits the proliferation and invasion of cells, promotes G2/M phase arrest and apoptosis, and exerts a therapeutic effect on LUAD by targeting MAPK1, which affects the Ras signaling pathway.

5 Conclusion

To summarize, through a combination of network pharmacological analysis and cell experiments, we revealed the mechanisms underlying the therapeutic effects of brusatol on LUAD. We found that brusatol inhibited the proliferation and invasion of A549 and H1299 cells by targeting MAPK1 and mediating the Ras signaling pathway, which induced apoptosis and cycle arrest. This study also provides a theoretical and experimental basis for using brusatol as an anticancer drug. Our findings provide new ideas for developing TCM as small-molecule inhibitors.

6 Figures and Tables

6.1 Figure 1

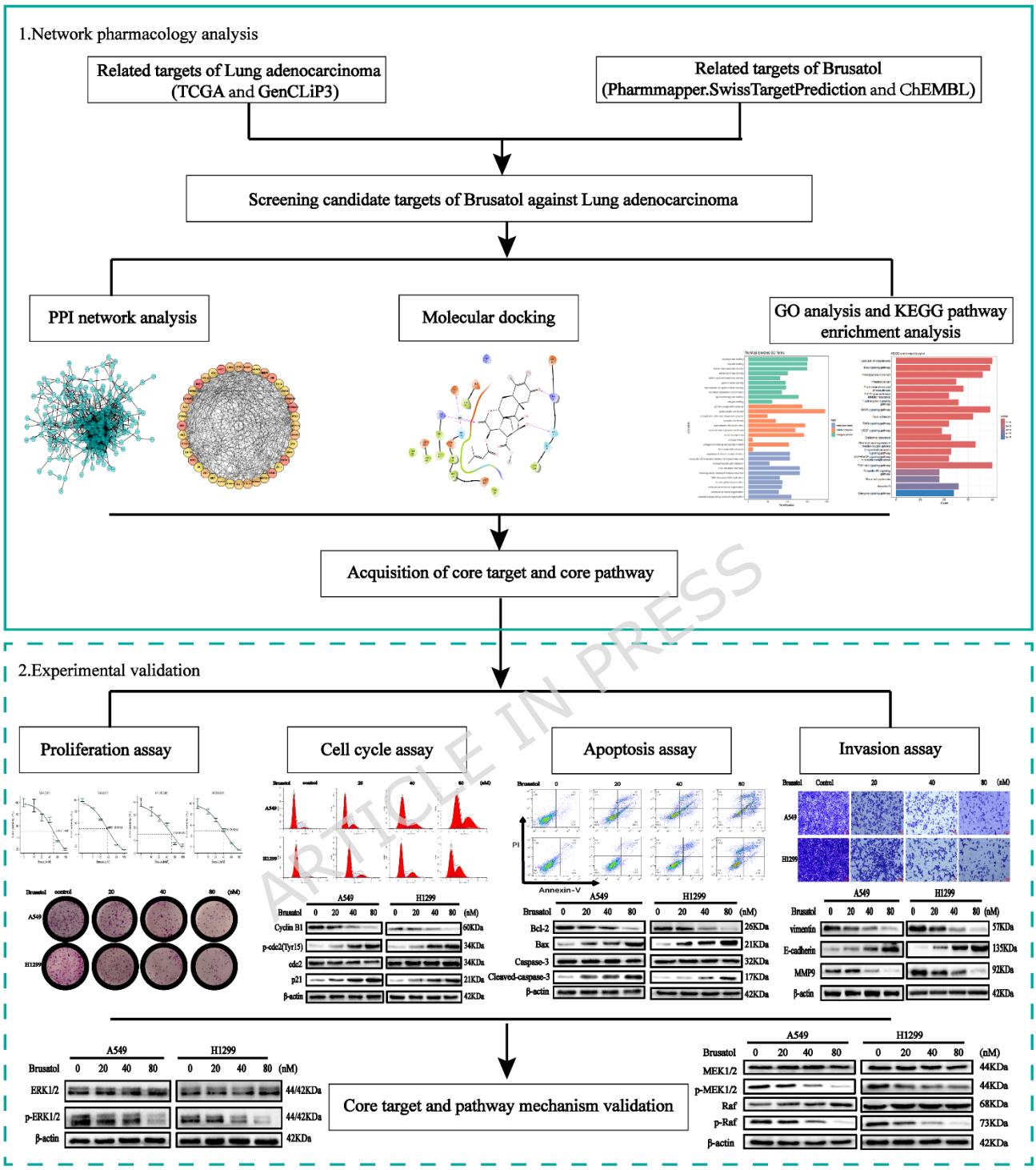

Figure 1. Workflow of the network pharmacology analysis and validation of brusatol against LUAD.

6.2 Figure 2

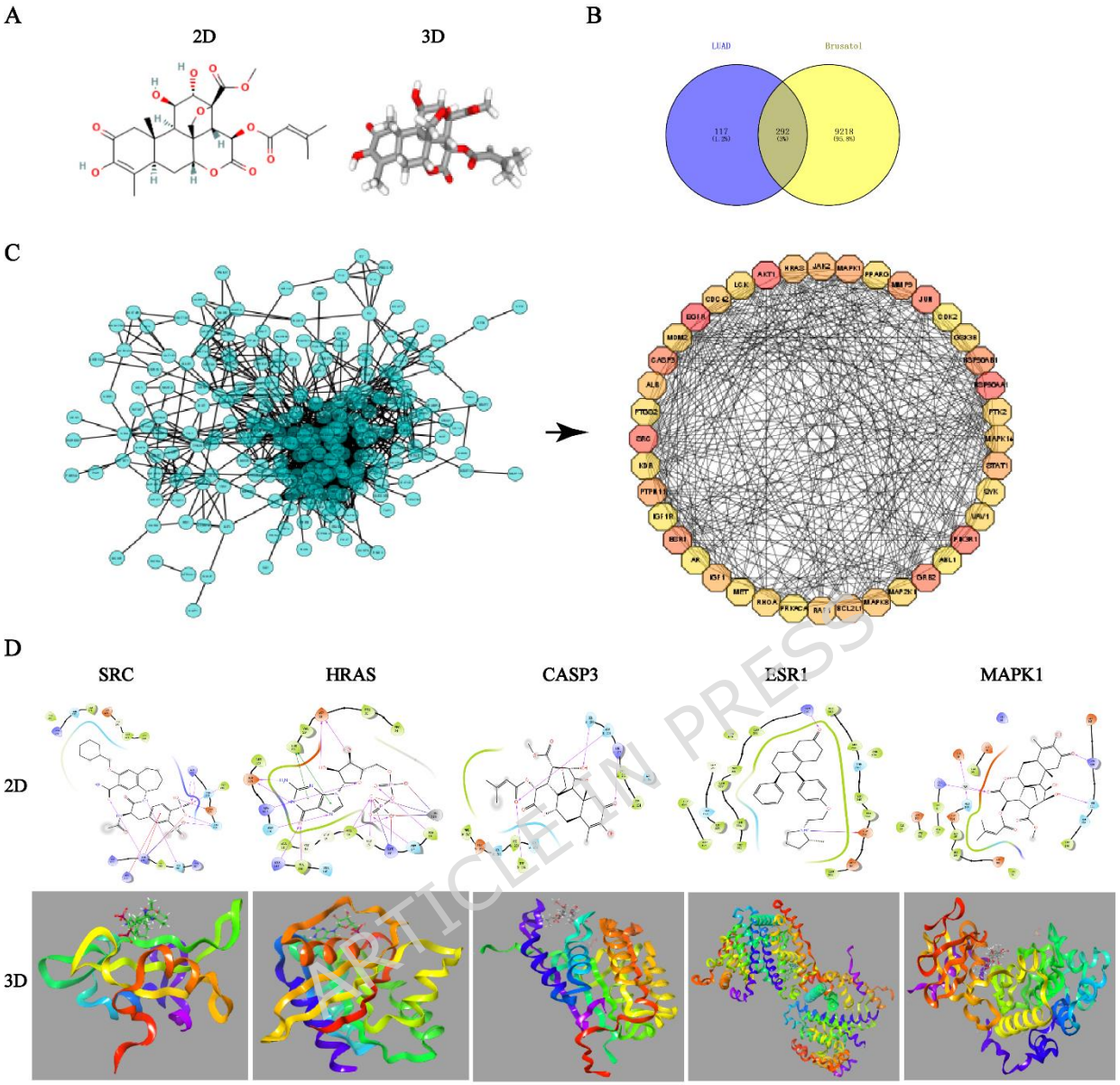

Figure 2. Network pharmacological analysis of brusatol. **(A)** The 2D and 3D structures of brusatol are shown. **(B)** The Venn diagram shows the 292 intersection targets of brusatol in lung adenocarcinoma (LUAD). **(C)** The protein-protein interactions of 292 intersecting genes were identified by the STRING platform, and the degree value of each node was calculated using the Cytoscape 3.8.0 software and the R software. The top 40 targets were visualized based on the size of the degree value. **(D)** The 2D and 3D structures of the molecular docking of key genes and brusatol are shown. **(E)** The top 10 terms in the GO analysis and the top 20 KEGG pathways are shown. The color scale indicates the different thresholds of p-values, and the length of the bar or the size of the dots represents the number of genes corresponding to each term.

6.3 Figure 3

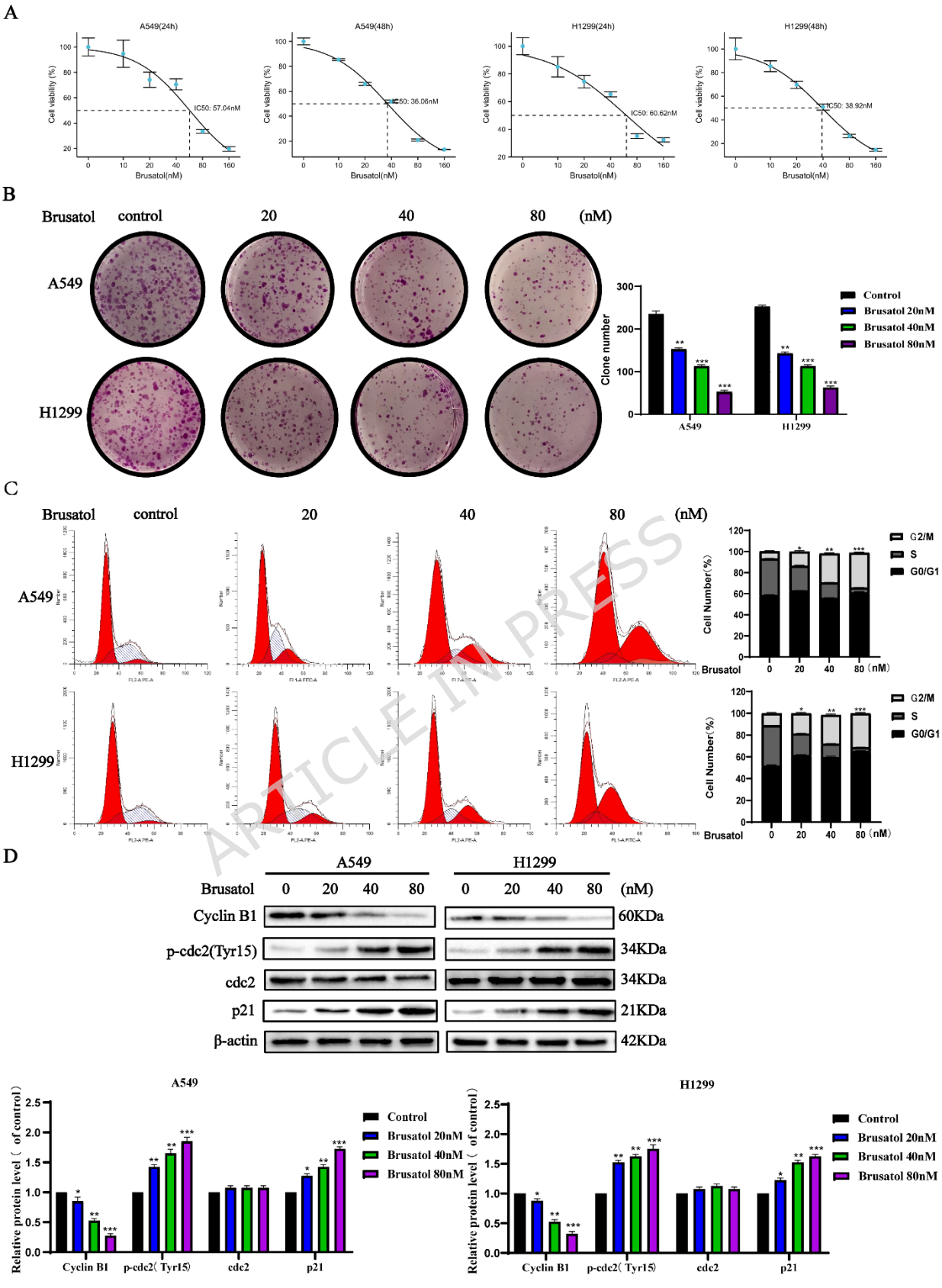

Figure 3. Brusatol inhibited the proliferation of LUAD cells. **(A)** MTT analysis of human LUAD cell lines (A549 and H1299 cells) after treatment with the indicated doses of brusatol for 24 h and 48 h. **(B)** Colony formation assays were performed on A549 and H1299 cells cultured with different concentrations (0, 20, 40, and 80 nM) of brusatol. The number of colonies formed was calculated and expressed as the mean ± standard deviation (SD) (n = 3). **(C)** Brusatol significantly inhibited the cell cycle progression of A549 and H1299 cells, arresting them in the G2/M phase, as shown by flow cytometry analysis (n = 3 per group). **(D)** The expression of cyclin B1 decreased, and the expression of p21 and p-cdc2 increased as brusatol concentration increased (n = 3 per group). The values are shown as the mean ± SD, *p < 0.05 and **p < 0.01 vs. the control.

6.4 Figure 4

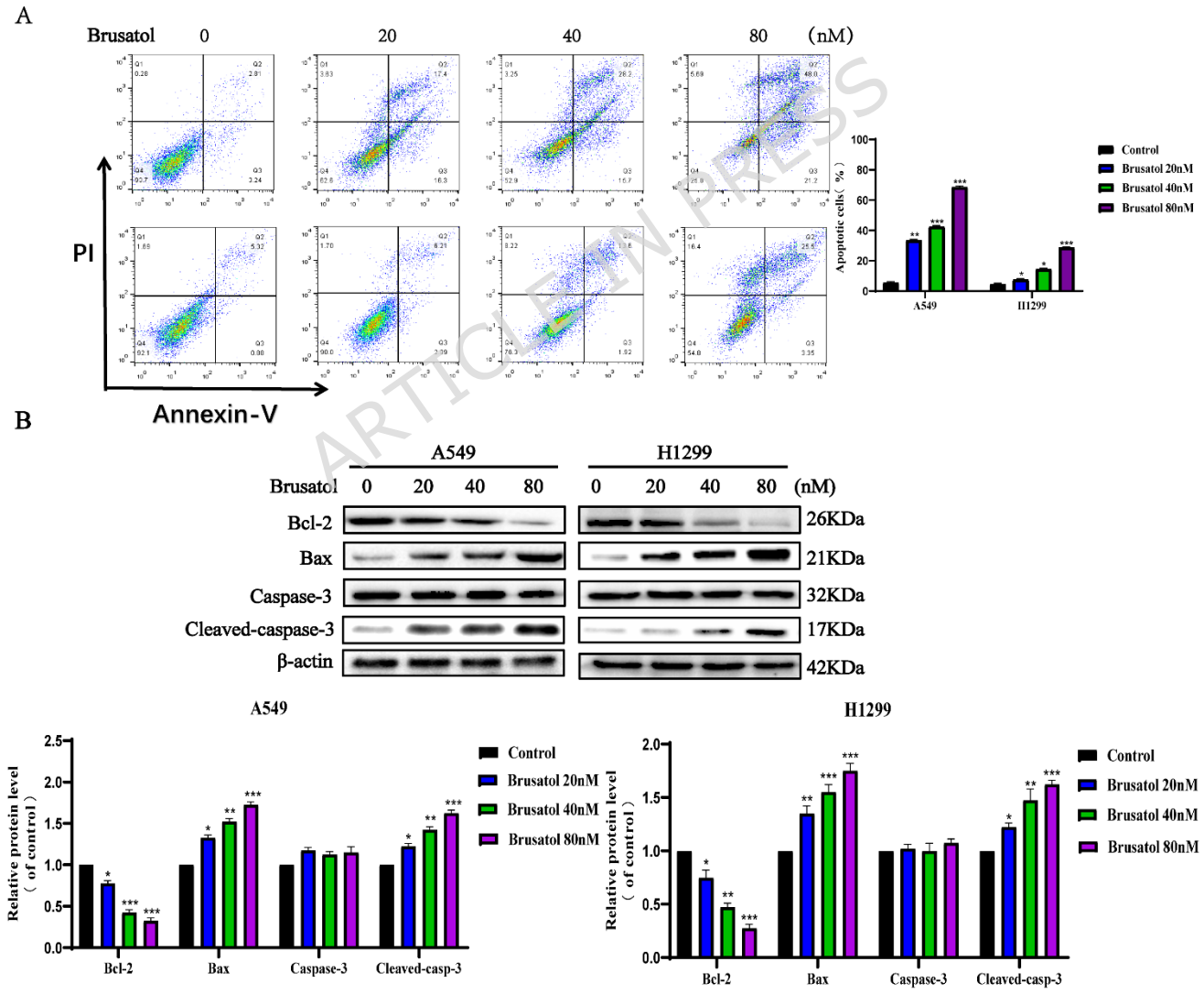

Figure 4. Brusatol significantly promoted LUAD apoptosis. **(A)** Flow cytometry analysis revealed that brusatol promoted early and late apoptosis in A549 and H1299 cells (n = 3 in each group). **(B)** The expression of Bcl-2 decreased, and the expression of Bax and cleaved caspase-3 increased with increasing brusatol concentration (n = 3 per group). The values are shown as the mean ± SD; *p < 0.05 and **p < 0.01 vs. the control.

6.5 Figure 5

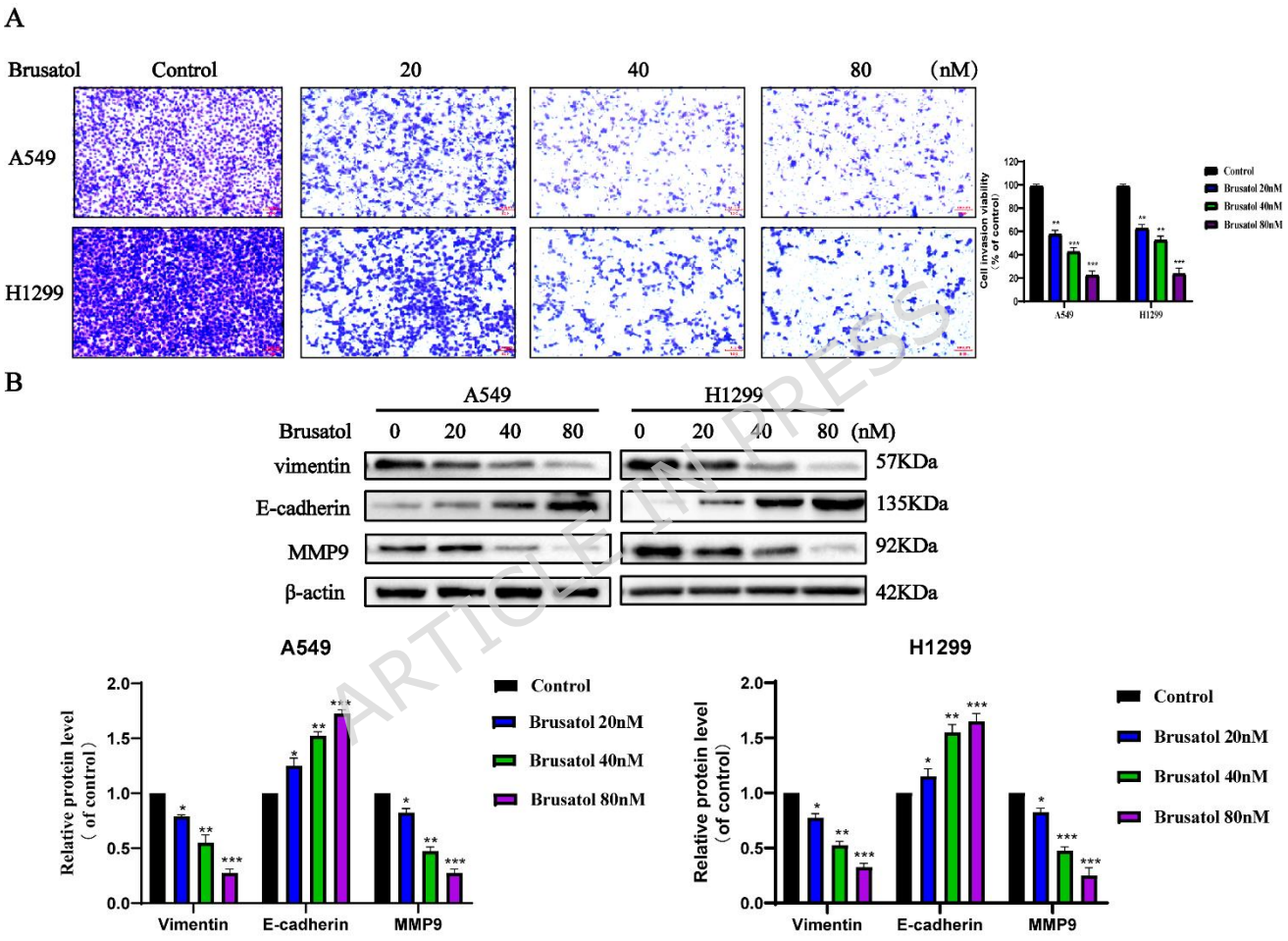

Figure 5. Brusatol inhibited the invasion of LUAD cells. **(A)** Transwell invasion assay of A549 and H1299 cells was conducted after brusatol treatment (100×); n = 6; *p < 0.05 and **p < 0.01 vs. the control. **(B)** The expression of MMP9 and vimentin decreased, and the expression of E-cadherin increased as brusatol concentration increased (n = 3 per group). The values are shown as the mean ± SD; *p < 0.05 and **p < 0.01 vs. the control.

6.6 Figure 6

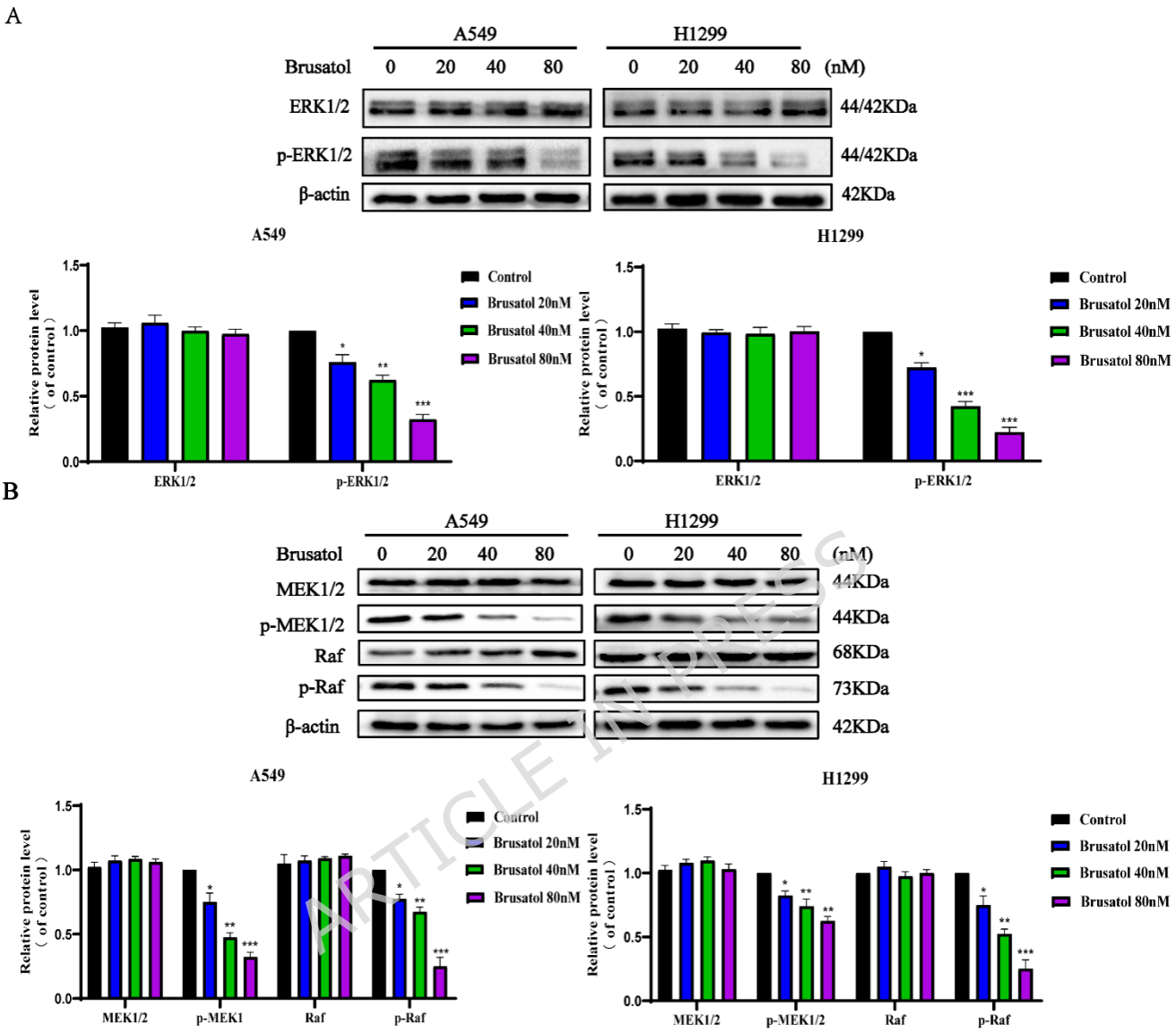

Figure 6. Molecular mechanisms underlying the therapeutic effects of brusatol on LUAD. **(A)** The expression of MAPK1 (ERK2) decreased as brusatol concentration increased. **(B)** The levels of Ras signaling pathway-related proteins were altered by brusatol treatment (n = 3 in each group). The values are shown as the mean ± SD; *p < 0.05 and **p < 0.01 vs. the control.

6.7 Table 1

Table 1. The top 40 intersecting genes

Rank	Name	Score
1	EGFR	63

2	AKT1	61
3	HSP90AA1	58
4	SRC	54
5	PIK3R1	42
6	JUN	41
7	GRB2	40
8	CASP3	38
9	ESR1	37
10	HSP90AB1	36
11	MMP9	34
12	MAPK1	33
13	PTPN11	32
14	STAT1	31
15	JAK2	29
16	BCL2L1	28
16	HRAS	28
16	IGF1	28
19	ALB	27
19	MAPK8	27
21	CDC42	26
21	RAF1	26
23	MAPK14	25
24	MDM2	24
24	PTK2	24
24	RHOA	24
27	VAV1	21
27	MAP2K1	21
27	GSK3B	21
27	LCK	21

6.8 Table 2

Table 2. Molecular docking of brusatol and key genes

Target	PDB ID	Docking Score
MAPK1	4g6o	-5.418
CASP3	1nme	-4.107
SRC	1fbz	-3.715
ESR1	7ujy	-2.47
HRAS	2quz	-2.384

7 References

[1] Wang N, Zhao G, Zhang Y, Wang X, Zhao L, Xu P, et al. A Network Pharmacology Approach to Determine the Active Components and Potential Targets of Curculigo Orchioides in the Treatment of Osteoporosis. Med Sci Monit 2017;23:5113–22. https://doi.org/10.12659/MSM.904264.

[2] AACR Centennial Series: The Biology of Cancer Metastasis: Historical Perspective | Cancer Research | American Association for Cancer Research n.d. https://aacrjournals.org/cancerres/article/70/14/5649/559515/AACR-Centennial-Series-The-Biology-of-Cancer (accessed December 8, 2025).

[3] Elgebaly SA, Hall IH, Lee KH, Sumida Y, Imakura Y, Wu RY. Antitumor Agents XXXV: Effects of Brusatol, Bruceoside A, and Bruceantin on P-388 Lymphocytic Leukemia Cell Respiration. Journal of Pharmaceutical Sciences 1979;68:887–90. https://doi.org/10.1002/jps.2600680727.

[4] Wong RS. Apoptosis in cancer: from pathogenesis to treatment. J Exp Clin Cancer Res 2011;30:87. https://doi.org/10.1186/1756-9966-30-87.

[5] Tang X, Fu X, Liu Y, Yu D, Cai SJ, Yang C. Blockade of glutathione metabolism in IDH1-mutated glioma. Mol Cancer Ther 2020;19:221–30. https://doi.org/10.1158/1535-7163.MCT-19-0103.

[6] Ren D, Villeneuve NF, Jiang T, Wu T, Lau A, Toppin HA, et al. Brusatol enhances the efficacy of chemotherapy by inhibiting the Nrf2-mediated defense mechanism. Proc Natl Acad Sci U S A 2011;108:1433–8. https://doi.org/10.1073/pnas.1014275108.

[7] Brusatol inhibits growth and induces apoptosis in pancreatic cancer cells via JNK/p38 MAPK/NF-κb/Stat3/Bcl-2 signaling pathway. Biochemical and Biophysical Research Communications 2017;487:820–6. https://doi.org/10.1016/j.bbrc.2017.04.133.

[8] Brusatol inhibits laryngeal cancer cell proliferation and metastasis via abrogating JAK2/STAT3 signaling mediated epithelial-mesenchymal transition. Life Sciences 2021;284:119907. https://doi.org/10.1016/j.lfs.2021.119907.

[9] Dai Z, Cai L, Chen Y, Wang S, Zhang Q, Wang C, et al. Brusatol Inhibits Proliferation and Invasion of Glioblastoma by Down-Regulating the Expression of ECM1. Front Pharmacol 2021;12:775680. https://doi.org/10.3389/fphar.2021.775680.

[10] Olayanju A, Copple IM, Bryan HK, Edge GT, Sison RL, Wong MW, et al. Brusatol provokes a rapid and transient inhibition of Nrf2 signaling and sensitizes mammalian cells to chemical

toxicity—implications for therapeutic targeting of Nrf2. Free Radic Biol Med 2015;78:202–12. https://doi.org/10.1016/j.freeradbiomed.2014.11.003.

[11] Chen H, Jiang T, Chen H, Su J, Wang X, Cao Y, et al. Brusatol reverses lipopolysaccharide-induced epithelial-mesenchymal transformation and induces apoptosis through PI3K/Akt/NF-κB pathway in human gastric cancer SGC-7901 cells. Anti-Cancer Drugs 2021;32:394. https://doi.org/10.1097/CAD.0000000000001022.

[12] Lee JH, Mohan CD, Deivasigamani A, Jung YY, Rangappa S, Basappa S, et al. Brusatol suppresses STAT3-driven metastasis by downregulating epithelial-mesenchymal transition in hepatocellular carcinoma. J Adv Res 2020;26:83–94. https://doi.org/10.1016/j.jare.2020.07.004.

[13] Chen Z, He B, Zhao J, Li J, Zhu Y, Li L, et al. Brusatol suppresses the growth of intrahepatic cholangiocarcinoma by PI3K/Akt pathway. Phytomedicine 2022;104:154323. https://doi.org/10.1016/j.phymed.2022.154323.

[14] Oh E-T, Kim CW, Kim HG, Lee J-S, Park HJ. Brusatol-Mediated Inhibition of c-Myc Increases HIF-1α Degradation and Causes Cell Death in Colorectal Cancer under Hypoxia. Theranostics 2017;7:3415–31. https://doi.org/10.7150/thno.20861.

[15] Cai SJ, Liu Y, Han S, Yang C. Brusatol, an NRF2 inhibitor for future cancer therapeutic. Cell Biosci 2019;9:45. https://doi.org/10.1186/s13578-019-0309-8.

[16] Feng R-M, Zong Y-N, Cao S-M, Xu R-H. Current cancer situation in China: good or bad news from the 2018 Global Cancer Statistics? Cancer Commun (Lond) 2019;39:22. https://doi.org/10.1186/s40880-019-0368-6.

[17] Ritchie ME, Phipson B, Wu D, Hu Y, Law CW, Shi W, et al. limma powers differential expression analyses for RNA-sequencing and microarray studies. Nucleic Acids Res 2015;43:e47–e47. https://doi.org/10.1093/nar/gkv007.

[18] Dai C, Ma Z, Si J, An G, Zhang W, Li S, et al. Hsa_circ_0007312 Promotes Third-Generation Epidermal Growth Factor Receptor-Tyrosine Kinase Inhibitor Resistance through Pyroptosis and Apoptosis via the MiR-764/MAPK1 Axis in Lung Adenocarcinoma Cells. J Cancer 2022;13:2798–809. https://doi.org/10.7150/jca.72066.

[19] Yan Z, Ohuchida K, Fei S, Zheng B, Guan W, Feng H, et al. Inhibition of ERK1/2 in cancer-associated pancreatic stellate cells suppresses cancer–stromal interaction and metastasis. J Exp Clin Cancer Res 2019;38:221. https://doi.org/10.1186/s13046-019-1226-8.

[20] Integrating signals from RTKs to ERK/MAPK | Oncogene n.d. https://www.nature.com/articles/1210394 (accessed December 8, 2025).

[21] Kanehisa M, Furumichi M, Sato Y, Matsuura Y, Ishiguro-Watanabe M. KEGG: biological systems database as a model of the real world. Nucleic Acids Res 2024;53:D672–7. https://doi.org/10.1093/nar/gkae909.

[22] Kanehisa M. Toward understanding the origin and evolution of cellular organisms. Protein Sci 2019;28:1947–51. https://doi.org/10.1002/pro.3715.

[23] Kanehisa M, Goto S. KEGG: Kyoto Encyclopedia of Genes and Genomes. Nucleic Acids Res 2000;28:27–30. https://doi.org/10.1093/nar/28.1.27.

[24] Luo M, Liang C. LncRNA LINC00483 promotes gastric cancer development through regulating MAPK1 expression by sponging miR-490-3p. Biol Res 2020;53:14. https://doi.org/10.1186/s40659-020-00283-6.

[25] Luteolin, a flavonoid, as an anticancer agent: A review. Biomedicine & Pharmacotherapy 2019;112:108612. https://doi.org/10.1016/j.biopha.2019.108612.

[26] Network pharmacology | Nature Biotechnology n.d. https://www.nature.com/articles/nbt1007-1110 (accessed December 8, 2025).

[27] Yuan C, Wang M-H, Wang F, Chen P-Y, Ke X-G, Yu B, et al. Network pharmacology and molecular docking reveal the mechanism of Scopoletin against non-small cell lung cancer. Life Sciences 2021;270:119105. https://doi.org/10.1016/j.lfs.2021.119105.

[28] Network pharmacology based virtual screening of active constituents of Prunella vulgaris L. and the molecular mechanism against breast cancer | Scientific Reports n.d. https://www.nature.com/articles/s41598-020-72797-8 (accessed December 8, 2025).

[29] He S, Wang T, Shi C, Wang Z, Fu X. Network pharmacology-based approach to understand the effect and mechanism of Danshen against anemia. Journal of Ethnopharmacology 2022;282:114615. https://doi.org/10.1016/j.jep.2021.114615.

[30] Network pharmacology: the next paradigm in drug discovery | Nature Chemical Biology n.d. https://www.nature.com/articles/nchembio.118 (accessed December 8, 2025).

[31] Molina JR, Yang P, Cassivi SD, Schild SE, Adjei AA. Non–Small Cell Lung Cancer: Epidemiology, Risk Factors, Treatment, and Survivorship. Mayo Clin Proc 2008;83:584–94. https://doi.org/10.4065/83.5.584.

[32] Jensen M, Engert A, Weissinger F, Knauf W, Kimby E, Poynton C, et al. Phase I study of a novel pro-apoptotic drug R-etodolac in patients with B-cell chronic lymphocytic leukemia. Invest New Drugs 2008;26:139–49. https://doi.org/10.1007/s10637-007-9106-z.

[33] McCubrey JA, Steelman LS, Chappell WH, Abrams SL, Wong EWT, Chang F, et al. ROLES OF THE RAF/MEK/ERK PATHWAY IN CELL GROWTH, MALIGNANT TRANSFORMATION AND DRUG RESISTANCE. Biochim Biophys Acta 2007;1773:1263–84. https://doi.org/10.1016/j.bbamcr.2006.10.001.

[34] Wang Y, Zhu W, Chen X, Wei G, Jiang G, Zhang G. Selenium-binding protein 1 transcriptionally activates p21 expression via p53-independent mechanism and its frequent reduction associates with poor prognosis in bladder cancer. J Transl Med 2020;18:17. https://doi.org/10.1186/s12967-020-02211-4.

[35] Targeting metastasis | Nature Reviews Cancer n.d. https://www.nature.com/articles/nrc.2016.25 (accessed December 8, 2025).

[36] Liu Y, Hu X, Han C, Wang L, Zhang X, He X, et al. Targeting Tumor Suppressor genes for Cancer Therapy. Bioessays 2015;37:1277–86. https://doi.org/10.1002/bies.201500093.

[37] Baritaki S, Militello L, Malaponte G, Spandidos DA, Salcedo M, Bonavida B. The anti-CD20 mAb LFB-R603 interrupts the dysregulated NF-κB/Snail/RKIP/PTEN resistance loop in B-NHL cells: Role in sensitization to TRAIL apoptosis. International Journal of Oncology 2011;38:1683–94. https://doi.org/10.3892/ijo.2011.984.

[38] The biology and management of non-small cell lung cancer | Nature n.d. https://www.nature.com/articles/nature25183 (accessed December 8, 2025).

[39] Schafer KA. The Cell Cycle: A Review. Vet Pathol 1998;35:461–78. https://doi.org/10.1177/030098589803500601.

[40] Toward personalized treatment approaches for non-small-cell lung cancer | Nature Medicine n.d. https://www.nature.com/articles/s41591-021-01450-2 (accessed December 8, 2025).

[41] Traditional Chinese medicine network pharmacology: theory, methodology and application. Chinese Journal of Natural Medicines 2013;11:110–20. https://doi.org/10.1016/S1875-5364(13)60037-0.

[42] Shields JM, Pruitt K, McFall A, Shaub A, Der CJ. Understanding Ras: 'it ain't over 'til it's over'. Trends in Cell Biology 2000;10:147–54. https://doi.org/10.1016/S0962-8924(00)01740-2.

[43] Wang M, Shi G, Bian C, Nisar MF, Guo Y, Wu Y, et al. UVA Irradiation Enhances Brusatol-Mediated Inhibition of Melanoma Growth by Downregulation of the Nrf2-Mediated Antioxidant Response. Oxid Med Cell Longev 2018;2018:9742154. https://doi.org/10.1155/2018/9742154.

Conflict of Interest

The authors declare that the research was conducted in the absence of any commercial or financial relationships.The authors have stated explicitly that there are no conflict of interest in connection with this article.

8 Author Contributions

Chunjiao Yang and Xin Jin contributed to conception and designed of the study. Shixiong Yang was responsible for manuscript revision. Dianzhu Pan performed the statistical analysis. Bo Jin wrote sections of the manuscript. Ye Zhang participated in the revision of the article.

All authors contributed to the article and approved the submitted version.

9 Funding

Not applicable.

10 Acknowledgments

Not applicable.

11 Supplementary Material

Not applicable.

12 Data Availability Statement

The original contributions presented in the study are included in the article/ Supplementary Material . Further inquiries can be directed to the corresponding author.

13 Disclosure

TCGA and HPA belong to public databases. The patients involved in the database have obtained ethical approval. Users can download relevant data for free for research and publish relevant articles. Our study is based on open source data, so there are no ethical issues and other conflicts of interest.The authors declare that the research was conducted in the absence of any com-mercial or financial relationships.The authors have stated explicitly that there are no conflict of interest in connection with this article.